

2016

Analysis of the Basigin Subset of the Immunoglobulin Superfamily Throughout the Mouse Lifespan

Tavia N. Hall

Suggested Citation

Hall, Tavia N., "Analysis of the Basigin Subset of the Immunoglobulin Superfamily Throughout the Mouse Lifespan" (2016). *UNF Undergraduate Honors Theses*. 7.
<https://digitalcommons.unf.edu/honors/7>

This Honors Thesis is brought to you for free and open access by the Student Scholarship at UNF Digital Commons. It has been accepted for inclusion in UNF Undergraduate Honors Theses by an authorized administrator of UNF Digital Commons. For more information, please contact [Digital Projects](#).

© 2016 All Rights Reserved

ANALYSIS OF THE BASIGIN SUBSET OF THE IMMUNOGLOBULIN
SUPERFAMILY THROUGHOUT THE MOUSE LIFESPAN

by

Tavia Nicole Hall

A thesis submitted to the Honors Program
in partial fulfillment of the requirements for
Honors in the Major – Biology

UNIVERSITY OF NORTH FLORIDA

HONORS PROGRAM

April, 2016

Unpublished work © Tavia Hall

Certificate of Approval

The thesis of Tavia Nicole Hall is approved:

Date

Judith D. Ochrietor, PhD
Mentor

Accepted for the Department of Biology:

Cliff Ross, PhD
Chairperson

Accepted for the Honors Program:

LouAnne B. Hawkins, MA
Coordinator, Office of Undergraduate Research

Dedication

I dedicate this thesis to

My parents, Susan and Robert

My siblings, Evan, Ryan, Brittany, Remington, Kylan and Alexander

My confidants, Ryan, Summer, and Luca

I would like to thank my family for their love and support and my friends for their unending understanding and encouragement. I owe great thanks to these people, who've contributed largely to who I am today and what I've been able to accomplish.

There are not words to express my gratitude for your infinite love and unwavering confidence in me.

Acknowledgements

I would like to thank my mentor and research supervisor, Dr. Judith D. Ochrietor, for her continued guidance, support, and commitment throughout my transformation from naïve student to student scholar. I am grateful to have worked with such a dependable, compassionate, and inspiring mentor. I would also like to thank the faculty of the University of North Florida Biology Department for the knowledge and skills they've provided me during my undergraduate career. As I continue into graduate school, I know I will think of them often – and probably contact them frequently. The preparation provided enables me to approach future endeavors in education with confidence.

This work was partially funded by the Office of Undergraduate Research through a Student Mentored Academic Research Team (SMART) Grant and a Transformational Learning Opportunity (TLO) Grant. I would like to express my appreciation for being awarded financial support to pursue these studies.

Table of Contents

List of Tables and Figures.....	vi
Abstract.....	ix
Chapter 1 - Introduction.....	1
Basigin Subset of Immunoglobulin Superfamily.....	2
Monocarboxylate Transporters.....	13
Chapter 2 - Materials and Methods.....	19
Isolation of Brain Tissue.....	19
RNA Extraction from Brain Tissue.....	19
SYBR Green Based q-RT-PCR.....	20
Chapter 3 - Results.....	24
Chapter 4 – Discussion.....	36
Chapter 5 -Conclusions.....	42
References.....	44
Vita.....	51

List of Tables and Figures

Figure 1.1 Astrocytes use glucose to produce pyruvate through glycolysis. A portion of the pyruvate produced is used in cellular respiration to produce large amounts of ATP. Glycolysis exceeds cellular respiration in astrocytes and the majority of the pyruvate is reduced to lactate to allow glycolysis to continue. Monocarboxylate transporters move the lactate out of the astrocyte into the neurons where it will be used as metabolic energy. Astrocytes provide neurons with glutamine to synthesize glutamate, which is taken up by astrocytes after being released by neurons. (Demetrius et al., 2015).....	3
Figure 1.2 General model of the Basigin subset of the IgSF molecule. All members of the Basigin subset are single pass proteins with a single transmembrane domain, multiple extracellular loop-like domains, and a cytoplasmic domain. (Gambon, 2011).....	5
Figure 1.3 Sequence alignment analysis of the transmembrane domains of the Basigin subset of the IgSF using Clustal O(1.2.1) multiple sequence alignment (http://www.ebi.ac.uk/Tools/msa/clustalo/). Colors indicate residues are small and hydrophobic (red), acidic (blue), basic (purple), or have hydroxyl, sulfhydryl, and amine linkages (green). Grey symbols below the alignment indicate single, fully conserved residues (*), conservation between groups with strongly similar properties (:), or conservation between groups with weakly similar properties (.).....	7
Figure 1.4 Ribbon models of the Basigin Subset of Immunoglobulin Superfamily (A) Extracellular domains of short-form Basigin with two Ig-like loop domains (Redzic et al., 2011). (B) Ribbon model of the third extracellular domain of long form Basigin (Redzic et al., 2011). (C) MCT-1 (blue and red) in association with transmembrane domain of ancillary protein Embigin (green). Extracellular domains of Embigin in this figure are found to the right of MCT-1. (Halestrap, 2012) (D) Extracellular domains of short-form Neuroplastin, Np55 (Owczarek et al., 2010). (E) Extracellular domains of long Np65 with three Ig-like loop domains (Owczarek et al., 2011).....	8
Figure 1.5 Basigin, Embigin, and Neuroplastin each possess two extracellular Ig-like domains and a glutamate (E) in the same position within the transmembrane domain. Isoforms of Basigin and Neuroplastin have an additional extracellular Ig-like domain formed through differential splicing. The short-forms of Basigin and Neuroplastin are indicated in the darker colored loops and the long-forms are indicated by the lighter colored loops at the amino terminus. Glycosylation sites, signified by the grey symbols, differ between the proteins. (Beesley et al., 2014).....	10

Figure 1.6 The proposed lactate shuttle in the brain. A shuttle complex similar to the one thought to exist within the mouse retina was proposed for the mouse brain. The shuttle consists of a complex of short-form Neuroplastin (purple structures) and MCT-1 (green ovals) on glial cells and a complex of long-form Neuroplastin (yellow structures) and MCT1 on neurons. The complex is thought to transport lactate from glial cells to neurons. (Adapted from Ochrietor and Linser, 2003).....	18
Table 2.1 Primers used for q-RT-PCR analyses of Basigin, Embigin, Neuroplastin and MCT-1.....	23
Figure 3.1 Standard curve of PCR products amplified using specialized primers for Basigin. Threshold values were set at the level of exponential amplification, and single product formation was verified using a melt curve analysis (data not shown). Curve was generated using varying concentrations of twelve-month brain RNA. The line equation was obtained by application of a linear trendline.....	25
Figure 3.2 Standard curve of PCR products amplified using specialized primers for Embigin. Threshold values were set at the level of exponential amplification, and single product formation was verified using a melt curve analysis (data not shown). Curve was generated using varying concentrations of twelve-month brain RNA. The line equation was obtained by application of a linear trendline.....	26
Figure 3.3 Standard curve of PCR products amplified using specialized primers for Neuroplastin gene products. Threshold values were set at the level of exponential amplification, and single product formation was verified using a melt curve analysis (data not shown). Curve was generated using varying concentrations of twelve-month brain RNA. The line equation was obtained by application of a linear trendline.....	27
Figure 3.4 Comparison of Basigin, Neuroplastin, and Embigin expression. Tissue was isolated via an accepted protocol at the ages indicated and RNA was isolated for use in quantitative reverse transcription polymerase chain reaction (q-RT-PCR) using primer sets specific for Basigin gene products, Neuroplastin gene products, and Embigin. The values obtained were normalized to 18s RNA. All runs were performed in triplicate using 100 ng total RNA, and the average nanograms of RNA was plotted. Error bars represent the coefficient of variance. The melt curves indicated that a single product was obtained for each primer set (data not shown).....	29

Figure 3.5 Comparison of Basigin expression over the mouse life span. Tissue was isolated via an accepted protocol at the ages indicated and RNA was isolated for use in quantitative reverse transcription polymerase chain reaction (q-RT-PCR) using primer sets specific for Basigin gene products. The values obtained were normalized to 18s RNA. All runs were performed in triplicate using 100 ng total RNA and the average nanograms of RNA was plotted. Error bars represent coefficient of variance. Significant difference between samples is indicated by the presence of bracket shown above and the corresponding *P* value. A melt curve analysis indicated that a single product was obtained (data not shown)..... 30

Figure 3.6 Comparison of Embigin expression over the mouse life span. Tissue was isolated via an accepted protocol at the ages indicated and RNA was isolated for use in quantitative reverse transcription polymerase chain reaction (q-RT-PCR) using primer sets specific for Embigin. The values obtained were normalized to 18s RNA. All runs were performed in triplicate using 100 ng total RNA and the average nanograms of RNA was plotted. Error bars represent the coefficient of variance. Significant difference between samples is indicated by the presence of bracket shown above and the corresponding *P* value. A melt curve analysis indicated that a single product was obtained (data not shown)..... 32

Figure 3.7 Comparison of Neuroplastin gene product expression over the mouse life span. Tissue was isolated via an accepted protocol at the ages indicated and RNA was isolated for use in quantitative reverse transcription polymerase chain reaction (q-RT-PCR) using primer sets specific for Neuroplastin gene products. The values obtained were normalized to 18s RNA. All runs were performed in triplicate using 100 ng total RNA and the average nanograms of RNA was plotted. Error bars represent the coefficient of variance. Significant difference between samples is indicated by the presence of bracket shown above and the corresponding *P* value. A melt curve analysis indicated that a single product was obtained (data not shown)..... 33

Table 3.1 Expression of monocarboxylate transporter 1 (MCT-1) in brain tissue over the mouse life span. Values represent average nanograms at the ages indicated. Statistically significant differences in expression compared to the six-month sample are indicated by the presence of an asterisk (*) and the corresponding *P* value. A melt curve analysis indicated that a single product was obtained (data not shown)..... 34

Abstract

The Immunoglobulin Superfamily (IgSF) is a subset of cellular adhesion molecules that are involved in regulation of a variety of cellular processes throughout the body. The purpose of this study was to quantify and compare the expression levels of the Basigin subset of the IgSF in the brain throughout the mouse life-span. This study is the first to compare the expression of Basigin, Embigin, and Neuroplastin, which form the Basigin subset of the IgSF. The expression levels of MCT-1, which is known to associate with Basigin in the neural retina, were also quantified to identify its role in brain tissue. Mouse brains were obtained using an accepted protocol and RNA was isolated for use in quantitative reverse transcription polymerase chain reaction (q-RT-PCR) using primer sets specific for Basigin, Neuroplastin gene products, Embigin, and MCT-1. The values obtained were normalized to 18s rRNA and standard curves were generated to extrapolate the quantity of RNA present in each sample. Neuroplastin had the highest level of expression of the members of the Basigin subset of the IgSF over time. This suggests that Neuroplastin gene products have a more prominent role in the structure and function of the mouse brain than the other two members of the Basigin subset. Although expression of Neuroplastin was relatively high in adult brain tissue, an exponential pattern of decreasing expression over time was observed. It is possible that the decrease in Neuroplastin expression observed in the brain tissue of aged individuals is associated with neural degeneration as a result of aging.

Chapter 1 – Introduction

The brain is a complex organ whose function has long been a centerpiece in scientific research. This enigma that works as the body's center for sensation, coordination, and intellectual activity has fascinated and bewildered researchers since first being studied over 2000 years ago. Knowledge of the complicated processes performed by the brain continues to grow as studies of the brain's many roles advance. The brain is responsible for maintaining behavioral and cognitive operations, as well as molecular and cellular processes (Bear et al., 2007). As such, it continuously requires a substantial amount of respiratory fuel to ensure its metabolic needs are being met.

Fully developed brains are largely glucose dependent (Tsacopoulos and Mangretti, 1996). Historically, it has been widely accepted that glucose was the primary metabolite within neural tissue; however, monocarboxylates are also used as an energy source by the brain (Tsacopoulos and Mangretti, 1996; Halestrap and Wilson, 2012). Ketone bodies are used in high quantities throughout the early stages of post-natal development (Daniel et al., 1977; Vannucci and Duffy, 1974), and neurons in culture show a preference for lactate over glucose (Bouzier-Sore et al., 2003). Studies on lactate as an energy source show post-ischemic tissues elect to use lactate over glucose and that these lactate-dependent tissues exhibit neuroprotective properties (Bergensen, 2007). Although lactate presence was once believed to indicate hypoxia within neural tissue, these findings suggest lactate supports neuronal activity (Pellerin, 2003).

Neurons preferentially use extracellular lactate produced through fermentation of pyruvate by specialized glial cells of the central nervous system (CNS; Itoh et al., 2003). These specialized glial cells, known as astroglia or astrocytes, are highly glycolytic; therefore, glycolysis outpaces aerobic respiration even when oxygen is abundant. To allow glycolysis to continue, the electron carrier NAD^+ is reformed through reduction of pyruvate to lactate. The resulting lactate is transported into neurons from astroglia (Figure 1.1, Demetrius et al., 2015). A transport system that moves lactate from the astrocytes to the neurons must be present to allow this lactate transfer to occur. Because members of the Basigin subset of the Immunoglobulin Superfamily (IgSF) are involved in lactate transport in many tissues, such as the neural retina, it is possible they may be involved in lactate transport to neurons.

Basigin Subset of the Immunoglobulin Superfamily

The Basigin subset of the IgSF is classified as cellular adhesion molecules (CAMs). CAMs are a specialized group of proteins comprised of Cadherins, Integrins, Immunoglobulins, Mucins, and Selectins (Lodish et al., 2000). Classified according to their biochemical structure, CAMs are found on cell membrane surfaces and are responsible for binding with other cells or with the extracellular matrix (ECM) to create complexes necessary for biochemical and cellular processes (Williams, 1987). The Basigin subset of the IgSF consists of glycoproteins that contain covalently-bonded carbohydrates within their extracellular domains (Muramatsu, 1994; Langnaese et al., 1997). They are

Graphic redacted, paper copy available upon request to home institution.

Figure 1.1 Astrocytes use glucose to produce pyruvate through glycolysis. A portion of the pyruvate produced is used in cellular respiration to produce large amounts of ATP. Glycolysis exceeds cellular respiration in astrocytes and the majority of the pyruvate is reduced to lactate to allow glycolysis to continue. Monocarboxylate transporters move the lactate out of the astrocyte into the neurons where it will be used as metabolic energy. Astrocytes provide neurons with glutamine to synthesize glutamate, which is taken up by astrocytes after being released by neurons. (Demetrius et al., 2015)

characterized by two sandwiched β -sheets and immunoglobulin-like loops resulting from cysteine disulfide bridges (Halaby and Mornon, 1998).

The Basigin gene products, Neuroplastin gene products, and Embigin make up the Basigin subset of the IgSF. These are single pass transmembrane proteins with cytoplasmic domains at the carboxy terminus and extracellular domains at the amino terminus (Figure 1.2). The structures of these proteins are similar and share a high proportion of their amino acid sequences.

The Basigin subset of the IgSF has high amino acid sequence identity (Fan et al., 1998b, Beesley et al., 2014). Basigin shares 28% of its amino acid sequence with Embigin (Miyachi et al., 1991) and around 40% of its amino acid sequence with the Neuroplastins (Beesley et al., 2014). Although the entire structure of these proteins is similar, the intracellular and transmembrane domains of the Basigin subset show a higher percentage of conservation than the extracellular domains (Beesley et al., 2014).

Sequence alignments of the transmembrane domains of the Basigin subset show that these domains have greater than 50% amino acid identity among all three Basigin subset members. The transmembrane domains of Embigin and Basigin share more than 52% of their sequence, whereas Embigin and Neuroplastin share 65% of their amino acid sequences in their transmembrane domains. The highest amount of sequence conservation is

Graphic redacted, paper copy available upon request to home institution.

Figure 1.2 General model of the Basigin subset of the IgSF molecule. All members of the Basigin subset are single pass proteins with a single transmembrane domain, multiple extracellular loop-like domains, and a cytoplasmic domain. (Gambon, 2011)

seen in the transmembrane domains of Neuroplastin and Basigin, which is conserved by more than 67% (Figure 1.3, Clustal Omega, Sievers et al., 2011).

There is less similarity among the amino acid sequences for the extracellular domains of the Basigin subset compared to the high level of conservation seen in the transmembrane domains. However, the structural similarity of the extracellular domains within the Basigin subset is still significant. The extracellular domains of the Basigin subset of the IgSF do not exhibit homology with any other proteins to the degree of that is seen within the subset (Fan et al., 1998b). After considering the folded protein models of the extracellular domains for these proteins, the similar morphology between these proteins is obvious.

Ribbon models of these proteins show the folding patterns and tertiary structures achieved *in vivo* (Figure 1.4). The extracellular domains of short-form Basigin (Figure 1.4 A, Redzic et al., 2011) are visibly similar to those of short-form Neuroplastin (Figure 1.4 B, Owczarek et al., 2010) and Embigin (Figure 1.4 C, Halestrap, 2012). Long-form Basigin (Figure 1.4 D, Redzic et al., 2011) and long-form Neuroplastin (Figure 1.4 E, Owczarek et al., 2011) show similar morphology in their third extracellular domains as well as similarity to the loop-like domains of the short-form proteins.

Emb	L	V	V	L	S	F	L	V	P	L	K	P	F	L	A	I	L	A	E	V	I	L	L	V	A	I	I	L	L	-					
Bas	-	-	-	-	-	-	-	-	-	-	M	A	A	L	W	P	F	L	G	I	V	A	E	V	L	V	L	V	T	I	I	F	I	Y	
Np	-	-	-	-	-	-	-	-	-	-	-	-	-	-	-	-	-	-	-	-	-	-	-	-	-	-	-	-	-	-	-	-	-	-	
											*	*	*	*	.	*	:	*	*	:	:	:	:	*	*	.	*	*	.	:					

Figure 1.3 Sequence alignment analysis of the transmembrane domains of the Basigin subset of the IgSF using Clustal O (1.2.1) multiple sequence alignment (<http://www.ebi.ac.uk/Tools/msa/clustalo/>). Colors indicate residues are small and hydrophobic (red), acidic (blue), basic (purple), or have hydroxyl, sulfhydryl, and amine linkages (green). Grey symbols below the alignment indicate single, fully conserved residues (*), conservation between groups with strongly similar properties (:), or conservation between groups with weakly similar properties (.). (Seivers et al., 2011)

Graphic redacted, paper copy available upon request to home institution.

Figure 1.4 Ribbon models of the Basigin subset of the Immunoglobulin Superfamily. **(A)** Extracellular domains of short-form Basigin (Redzic et al., 2011). **(B)** Extracellular domains of short-form Neuroplastin, Np55 (Owczarek et al., 2010). **(C)** MCT-1 (blue and red) in association with the transmembrane domain of the ancillary protein Embigin (green). Extracellular domains of Embigin are found to the right of MCT-1. (Halestrap, 2012) **(D)** Ribbon model of the third extracellular domain of long form Basigin (Redzic et al., 2011). **(E)** Extracellular domains of long-form Neuroplastin, Np65 with three Ig-like loop domains (Owczarek et al., 2011).

Basigin

Basigin is known by different names in different species, including CD147, 5A11, HT7, neurothelin, and EMMPRIN (reviewed in Miyauchi et al., 1991).

These proteins have high amino acid sequence identity even though they are found in different species (Toyama et al., 1999). The Basigin gene produces a transcript with eight exons that generates two different gene products through differential splicing. Basigin plays an important role in neuronal processes affecting vision, behavior, and olfaction (Ochrietor et al., 2002, Igakura et al., 1996, Fan et al., 1998a).

Basigin-1 is the short-form gene product with two Ig-like extracellular domains (Figure 1.5, Beesley et al., 2014). Basigin-1 is made up of 260 amino acids and is 45 kDa in size after glycosylation (Fan et al., 1998a). It is expressed ubiquitously throughout the body and is involved in various processes including spermatogenesis and tumorigenesis (Ochrietor et al., 2003; Nakai et al., 2006; Kanekura and Chen, 2010; Yan et al., 2005). In the neural retina, Basigin-1 is expressed by Müller glial cells and the retina pigmented epithelium (Ochrietor et al., 2003). Basigin-1 expression is found in neuroblasts, but levels decrease over time so that very little is found in adult neuroblasts (Fan et al., 1998a). Additionally, Basigin-1 is differentially expressed in different regions of the brain (Fan et al., 1998a).

Graphic redacted, paper copy available upon request to home institution.

Figure 1.5 Basigin, Embigin, and Neuroplastin each possess two extracellular Ig-like domains and a glutamate (E) in the same position within the transmembrane domain. Basigin and Neuroplastin can have an additional extracellular Ig-like domain formed through differential splicing. The short-forms of Basigin and Neuroplastin are indicated in the darker colored loops and the long-forms are indicated by the lighter colored loops at the amino terminus. Glycosylation sites, signified by the grey symbols, differ between the proteins. (Beesley et al., 2014)

The splice variant Basigin-2 is known as the long-form gene product and has three Ig-like extracellular domains (Figure 1.5, Beesley et al., 2014). Basigin-2 includes the 1A exon, adding 116 amino acids and increasing the size to 50 kDa (Ochrietor et al., 2003). Basigin-2 is expressed solely in the photoreceptors of the neural retina (Ochrietor et al., 2003). Its localized expression pattern suggests that it plays a specialized role in this tissue.

Mice without functional Basigin display several abnormalities. Basigin null mice are blind at the time of eye opening and display complete photoreceptor degradation by one year of age (Ochrietor and Linser, 2004). Mice with Basigin deletion also show a decrease in pain tolerance (Naruhashi et al., 1997) and are reproductively sterile (Igakura et al., 1998).

Embigin

Embigin homologs are also present in a wide variety of species (Guenette et al., 1997). There is only one form of Embigin and it has a molecular weight of 30 kDa when unglycosylated (Fan et al., 1998b). It possesses two extracellular Ig-like domains (Figure 1.5, Ozawa et al., 1988). Embigin responds to changes in the cellular environment to regulate cell growth and differentiation (Guenette et al., 1997). Embigin is preferentially expressed during day five through ten of embryogenesis and is involved in regulation during cellular differentiation (Fan et al., 1998b). Embigin expression is found in all tissue, but is weakly expressed in adult tissues. Adult brain tissue exhibits lower Embigin expression relative to other adult tissues (Fan et al., 1998b).

Embigin has also been found to play an important role in mediation of the neuromuscular junction (Lain et al., 2009). Forced overexpression of Embigin in adult tissue results in nerve terminal sprouting at the motor endplate (Lain et al., 2009). Upregulation of Embigin is also seen individuals that are paralyzed (Llano-Diez et al., 2011). Embigin, like Basigin, plays a role in tumorigenesis and supports cancer development as increased Embigin expression is seen in embryonal carcinoma cells (Huang et al., 1990).

Neuroplastin

Neuroplastin is similar to Basigin in that it has multiple gene products that result from differential splicing. The junction between two neurons across which a nerve impulse is passed, the neural synapse, is enriched with both Neuroplastin gene products, but they show different physiological functions, expression patterns, and developmental profiles in the brain (Beesley et al., 2014). The Neuroplastins are involved in mediating neurite outgrowth, neuronal plasticity, and synaptogenesis (Beesley et al., 2014).

The Neuroplastin gene products are named for their molecular weights. The short-form Neuroplastin is 55 kDa and is known as Np55. Similarly, the long-form Neuroplastin is known as Np65 and is 65 kDa (Langnaese et al., 1998). Np55 has two extracellular Ig-like domains and Np65 has three extracellular Ig-like domains (Figure 1.5, Beesley et al., 2014). Np55 is found in tissues throughout the body, but is predominately expressed in nervous tissue (Wilson et al., 2013).

Long-form Neuroplastin, Np65, is brain specific and is expressed only in neural tissue (Wilson et al., 2013). Np65 is involved in regulating synaptic structure and function in the brain (Beesley et al., 2014). Like the localized expression of Basigin-2 in the photoreceptors of the neural retina, the restricted expression of Np65 in brain suggests that it plays an important role in this tissue.

Monocarboxylate Transporters

Monocarboxylate transporters, or MCTs, are transport proteins that are responsible for the movement of monocarboxylates, such as lactate, pyruvate, and ketone bodies (Halestrap and Prince, 1999). MCTs play a role in shuttling monocarboxylates across the plasma membrane between two adjacent cells (Kirk et al., 2000). The purpose of this transfer is to provide the receiving cell with the monocarboxylate for use in generating metabolic energy (Halestrap, 2012).

Members of the MCT family have twelve helical transmembrane domains and a large intracellular cytosolic loop region. Because they are made up of a multitude of coiled coils, they are hydrophobic in nature (Figure 1.4 C). As such, MCTs are highly compatible with the lipid bilayer and are easily embedded within the plasma membrane (Halestrap, 2012).

The Basigin subset of the IgSF associates with monocarboxylate transporters and are involved in a variety of cellular processes (Halestrap, 2012). For example, synaptogenesis, photoreceptor metabolism, and neuromuscular

regeneration rely heavily on the complexes produced through association of the Basigin subset of the IgSF with MCTs (Wilson et al., 2013; Ochrietor and Linser, 2004; Lain et al., 2009). The neural synapse is affected by IgSF proteins and other CAMs through mediated guidance cues (Shen, 2004; Carillo et al, 2015), and photoreceptors degrade over time without the presence of the Basigin-MCT-1 complex (Philp et al., 2003a).

MCT-1

Like other members of the MCT family, MCT-1 moves lactate across the cell membrane of neighboring cells through proton linked co-transport; however, MCT-1 requires an accessory protein to locate to the cell surface and properly perform its function; MCT-1 must first bind to a member of the Basigin subset of the IgSF (Kirk et al., 2000; Wilson et al., 2002; Philp et al., 2003a). Found in many tissues throughout the body, MCT-1 is widely distributed and is frequently co-expressed with Basigin (Philp et al., 2003a; Clamp et al., 2004; Wilson et al., 2009). MCT-1 has a moderate affinity for Basigin and forms a complex through hydrophobic interactions (Finch et al., 2009; Howard et al., 2010).

MCT-1 is expressed throughout the neural retina in Müller glia as well as in photoreceptors (Philp et al., 2003b). In the neural retina, MCT-1 binds to Basigin and forms a complex that provides photoreceptors with lactate for use as metabolic fuel (Philp et al., 2003a; Finch et al., 2009). In this tissue, Basigin serves as the accessory protein to MCT-1 and moves it to the cell membrane.

Metabolism

The Müller glia in retinal tissue, like the astroglia in neural tissue, are highly glycolytic, meaning that the rate of glycolysis out-paces the rate of aerobic respiration, even in the presence of oxygen (Pellerin, 2005). Because glycolysis is so active in this tissue, the pyruvate produced through glycolysis is fermented to lactate to regenerate the electron carriers NAD^+ and allow glycolysis to continue. The lactate produced by the Müller glia is used by the photoreceptors as an energy source (Suzuki et al., 2011). A study on the neural retina suggests that the Basigin-MCT-1 complex at the plasma membrane forms a shuttle that allows lactate produced through fermentation of pyruvate to be moved from supporting glial cells to photoreceptors (Ochrietor and Linser, 2004; Philp et al., 2003a).

This shuttle is formed by both the long-form and short-form Basigin gene products. Short-form Basigin and MCT-1 complex and move to the plasma membrane of Müller glial cells, while long-form Basigin and MCT-1 complex and move to the plasma membrane of photoreceptors. These complexes in Müller glia and photoreceptors come together to form what is known as the lactate metabolon. Through this metabolon, lactate can be shuttled from the supporting Müller glia to the adjacent photoreceptors.

Basigin null mice are blind from the time of opening (Hori et al., 2000; Ochrietor et al., 2002). Because there is an absence of functional Basigin in Basigin null mice, the lactate metabolon is not formed (Ochrietor and Linser,

2004; Philp et al., 2003a). In these mice, MCT-1 transcript levels are upregulated at post-natal day 20 in Basigin null mice, however, protein expression at the membrane is decreased; MCT-1 is not found at the plasma membrane but is trapped in vesicles within the cell (Philp et al., 2003a). In the absence of MCT-1 at the membrane, photoreceptors do not receive metabolic energy and cannot function, resulting in blindness (Philp et al., 2003a; Ochrietor et al. 2001). By one year of age, the photoreceptors of Basigin null mice have fully degenerated due to the unavailability of the lactate required for function and preservation of these cells (Ochrietor et al. 2001; Ochrietor and Linser, 2004).

As previously discussed, astroglia produce lactate that is used by neurons preferentially over glucose. Because neurons use lactate that is produced in neighboring glial cells, a lactate metabolon similar to the one found in the retina is hypothesized to exist in brain tissue (Figure 1.6). However, the ancillary protein responsible for MCT-1 transport to the cell membrane in brain tissue is not known and the complete mechanism is not yet understood. Unlike in retina, there are no changes in MCT-1 membrane-associated expression in the brains of Basigin null mice, (J. Ochrietor, unpublished results). The increased pain sensitivity and as well as the decreased olfactory and visual sensitivity observed in Basigin null mice suggest that Basigin plays a role in neural tissue (Igakura et al., 1996; Naruhashi et al., 1997). However, these deficiencies are inconsistent with the neural deficits that would be expected in the absence of the primary ancillary protein for MCTs in brain tissue. Mice lacking the primary accessory protein required for relocation of MCTs to the membrane of neurons and, by

extension, responsible for providing metabolic energy to these neurons, would likely show much more extensive and comprehensive neural deficits. Inability to provide metabolic energy to neural tissue would affect every neural system, not only those systems that are affected in the Basigin null mice. Therefore, another protein must be responsible for chaperoning the transporter to the membrane in this tissue.

The expression patterns of the Neuroplastins in the brain are analogous to the expression patterns of the Basigins in the neural retina. This suggests that the Neuroplastins may play a role in brain tissue that is similar to the role of the Basigins in retina. Additionally, the structure of Neuroplastin is similar to Basigin, which suggests that it may associate with MCT-1 and function as its ancillary protein in this tissue (Beesley et al., 2014).

The purpose of the present study was to quantify the expression levels of Basigin, Embigin, Neuroplastin gene products, and MCT-1 in the brain at points throughout the mouse life time. This study also analyzed and compared the expression levels of Basigin, Embigin and Neuroplastin to identify changes in expression patterns over time in the mouse. This is the first study to simultaneously study the expression of all three members of the Basigin subset of the IgSF in the mouse brain.

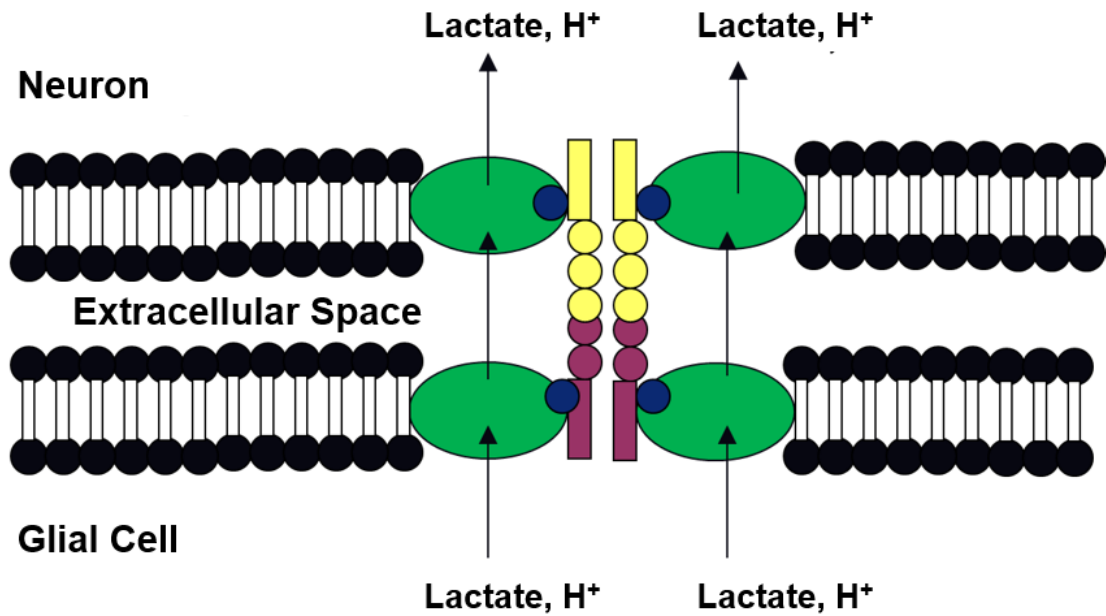


Figure 1.6 The proposed lactate shuttle in the brain. A shuttle complex similar to the one thought to exist within the mouse retina was proposed for the mouse brain. The shuttle consists of a complex of short-form Neuroplastin (purple structures) and MCT-1 (green ovals) on glial cells and a complex of long-form Neuroplastin (yellow structures) and MCT1 on neurons. The complex is thought to transport lactate from glial cells to neurons. (Adapted from Ochrietor and Linser, 2004)

Chapter 2 – Materials and Methods

Isolation of Brain Tissue and RNA Extraction

All animal procedures were approved by the UNF Institutional Animal Care and Use Committee (IACUC) and were in accordance with the American Veterinary Medical Association (AMVA). Mice (C57J/Bl – 129 hybrid [Igakura et al., 1998]) at one month of age, six months of age, and one year of age (three at each age) were euthanized and the brains were immediately isolated and rinsed with phosphate buffered saline (PBS, Amresco, Solon, OH). Each brain tissue sample was divided into left and right hemispheres in PBS. One hemisphere was used for RNA isolation and the other was stored at -80 °C.

RNA Extraction from Brain Tissue

RNA was isolated from each tissue sample using TRI Reagent (Molecular Research Center, Inc., Cincinnati, OH). The brain tissue was combined with 250 μ l TRI Reagent and homogenized using a motorized pestle (FisherBrand, Waltham, MA). The mixture was incubated at 25°C for 5 min. Chloroform (0.2 ml, Fisher Scientific, Pittsburgh, PA) was added and distributed through vigorous shaking, followed by incubation at 25 °C for approximately 10 min. The mixture was centrifuged at 12,000 \times g for 15 min. The upper aqueous phase containing the RNA was placed into a new microcentrifuge tube; the remaining biological material was discarded. RNA was precipitated by adding room temperature isopropanol (0.5 ml) to the solution, incubating at 25°C for approximately 10 min,

and centrifugation at 12,000 \times g for 8 min. The supernatant was discarded and the RNA pellet was washed with 1 ml of ice cold 75% ethanol. The pellet was re-suspended by passing it through a micropipette tip and reformed by centrifugation at 7,500 \times g for 5 minutes. The ethanol wash was removed and the pellet was briefly air dried. The RNA pellet was re-suspended in 100 μ l of Milli-Q water and incubated at 57°C for 15 min.

The concentrations of the RNA samples were determined using spectrophotometry. A 1:20 dilution of each RNA sample was prepared in Milli-Q water (100 μ l total volume) and transferred into individual wells of a UV-compatible plate (Corning Inc., Corning, NY). The absorbance of each sample was measured at 260 nm and 280 nm using a Bio-Tek plate reader (Winooski, VT). The concentrations of each sample were calculated considering one unit of absorbance at 260 nm equal to 40 μ g/mL of RNA. The purity of the isolated RNA samples was determined by calculating the ratio of the absorbance at 260 nm to that at 280 nm.

SYBR Green Based q-RT-PCR

For quantitative reverse transcription-polymerase chain reaction (q-RT-PCR), 100 ng of RNA was combined with primers specific for Basigin gene products, Embigin, Neuroplastin gene products, MCT-1, or 18s rRNA (1.0 μ l of forward primer and 1.0 μ l of reverse primer), 0.5 μ l of iScript Reverse Transcriptase (Bio-Rad Laboratories, Hercules, CA), 1.0 μ l of random hexamers

(Amersham Corporation, Piscataway, NJ), and 12.5 μ l of SYBR Green (Bio-Rad Laboratories) in 25 μ l total volume. Table 2.1 shows the primer sequences and concentrations used. Reactions were run in triplicate for each RNA sample in using a CFX Connect™ iCycler (Bio-Rad Laboratories) and analyzed using the associated software. The cycling parameters included 50 °C for 10 min, 95 °C for 5 min, and 40 cycles of 95 °C for 6 seconds and 55 °C for 18 seconds. A melt curve analysis was performed at the completion of amplification. Threshold values were compared to a standard curve for each primer set, and the amount of RNA for Basigin, Embigin, Neuroplastin, and MCT-1 was normalized to 18s rRNA.

Standard curves were generated for the Basigin subset of the IgSF members using known concentrations of RNA and primers for each molecular species. RNA from twelve-month brain tissue was prepared in samples of increasing concentration from zero to four hundred nanograms. Reactions were prepared using the procedure and parameters explained above. The threshold values and the log nanograms of the known RNA concentrations were plotted with a linear trendline using Microsoft Excel software. The nanograms of RNA for each sample was extrapolated using the line equation given by the standard curve for each gene product.

The average nanograms of RNA for each age and gene product studied was plotted using Microsoft Excel software. The data were reported as the mean RNA transcript level in nanograms for the specified age of each gene product.

The error bars represent the coefficient of variance for each sample. Pairwise comparisons between the one-month, six-month, and twelve-month samples were performed for each molecular species. The variance between samples was compared using an F-test to determine scedasticity. A t-test was performed to identify statistically significant changes between the ages studied for each gene product. Data was analyzed by a Student's t-test (unpaired) or a paired t-test depending on the variance between the two samples.

Table 2.1 Primers used for q-RT-PCR analyses of Basigin, Embigin, Neuroplastin and MCT-1.

Primer	Sequence	Concentration
MCT-1 Forward	5' TGG GCT TGT GGC GTG AT 3'	50 μ M
MCT-1 Reverse	5' TTG ATG CCC ATG CCA ATG 3'	50 μ M
Basigin Forward – pET-102-TM Fwd	5' CAC CAT GGC AGC CCT CTG GCC C 3'	50 μ M
Basigin Reverse – pET-102-TM RV	5' ATA GAT AAA GAT GAT GGT AAC CAA CA 3'	50 μ M
Embigin Forward – pETEmbTMF	5' CAC CCT GGT GCC CCT CAA GCC A 3'	100 μ M
Embigin Reverse – pETEmbTMRV	5' ACA AAG CAG AAT GAT GGC CAC CA 3'	100 μ M
Neuroplastin Forward – Np TM Fwd	5' CAC CCT TGC CCC ACT TTG GCC TT 3'	100 μ M
Neuroplastin Reverse – Np TM RV	5' ATA CAC AAC AAT GAT CAC CAC AAG G 3'	100 μ M

Chapter 3 – Results

The purpose of the present study was to analyze the expression of the members of the Basigin subset of the IgSF and MCT-1 over time in the mouse brain. This was accomplished via q-RT-PCR. RNA from one-month, six-month, and twelve-month brain tissue samples was isolated using an accepted protocol and used in q-RT-PCR. Specific primer sets for Basigin, Neuroplastin gene products, Embigin, and MCT-1 were used for amplification. Threshold values were set at the point of exponential amplification, and a melt curve analysis was performed to verify the presence of only one product. The values were normalized to 18s RNA, and the amount of transcript in each sample was calculated.

Standard curves for Basigin, Embigin, and Neuroplastin were generated and used to quantify the amount of PCR product formed in each reaction. The amount of MCT-1 was determined using an existing standard curve (Clamp et al., 2004). Similarly, the amount of 18s rRNA was also determined using an existing standard curve (Ochrietor et al., 2003). The concentration of RNA for each sample was extrapolated using the line equation given by application of a linear trendline to the standard curves generated from the collected data. The coefficient of determination for the Basigin standard curve was found to be 0.912 (Figure 3.1). The standard curve for Embigin had a coefficient of determination equal to 0.778 (Figure 3.2), and 0.924 was the coefficient of determination given by the Neuroplastin standard curve (Figure 3.3).

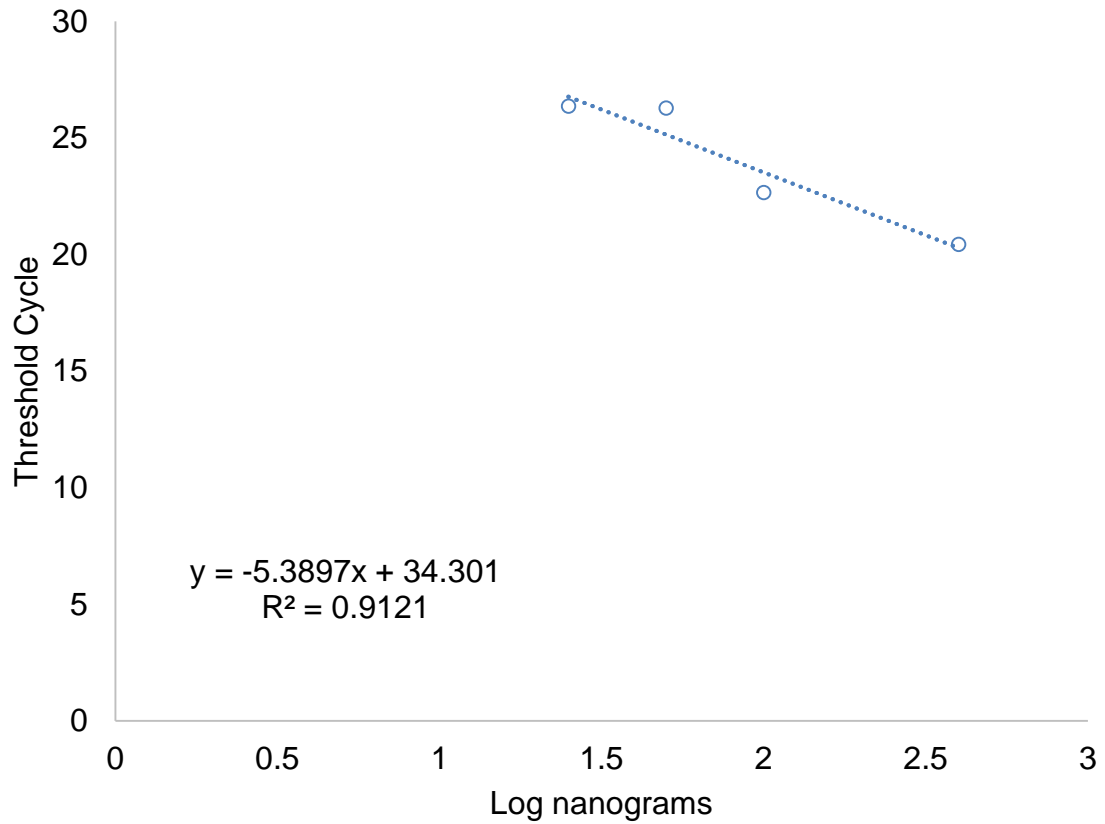


Figure 3.1 Standard curve of PCR products amplified using specialized primers for Basigin. Threshold values were set at the level of exponential amplification, and single product formation was verified using a melt curve analysis (data not shown). The curve was generated using varying concentrations of twelve-month brain RNA. The line equation was obtained by application of a linear trendline.

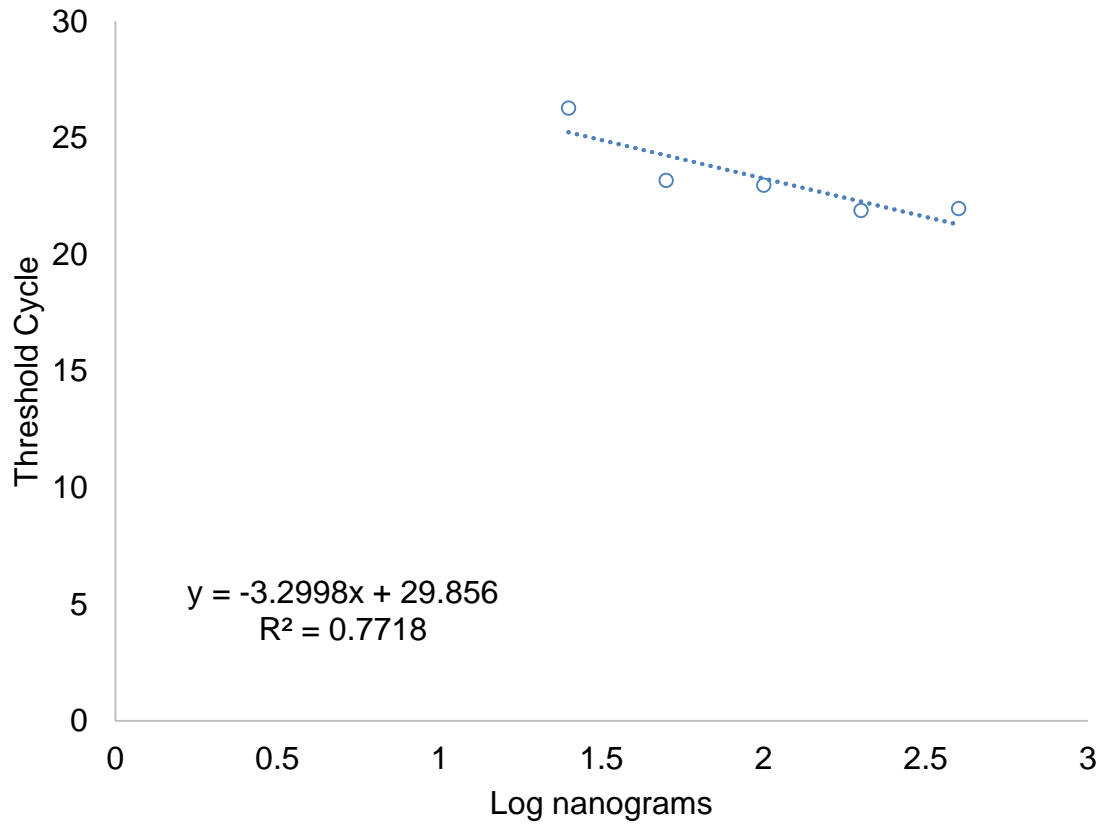


Figure 3.2 Standard curve of PCR products amplified using specialized primers for Embigin. Threshold values were set at the level of exponential amplification, and single product formation was verified using a melt curve analysis (data not shown). The curve was generated using varying concentrations of twelve-month brain RNA. The line equation was obtained by application of a linear trendline.

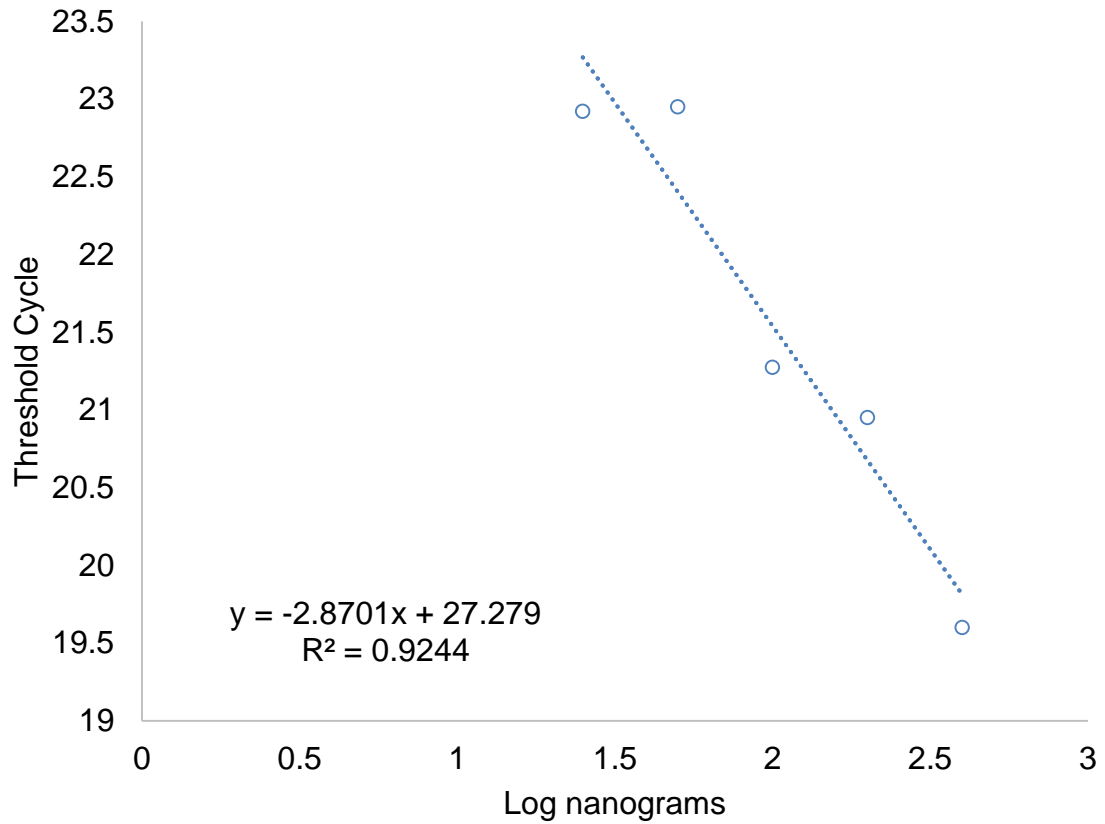


Figure 3.3 Standard curve of PCR products amplified using specialized primers for Neuroplastin gene products. Threshold values were set at the level of exponential amplification, and single product formation was verified using a melt curve analysis (data not shown). The curve was generated using varying concentrations of twelve-month brain RNA. The line equation was obtained by application of a linear trendline.

Once standard curves for transcript expression were generated for each of the primer sets, the expression levels of Basigin, Embigin, and Neuroplastin were compared. The normalized average nanograms of RNA for each molecular species was plotted and the error bars represent the coefficient of variance. The one-month brain tissue sample had the highest expression of all three of the Basigin subset members studied, when compared to the adult tissues (Figure 3.4). At all three time points, Neuroplastin had the highest expression of all the Basigin subset of the IgSF. Basigin was expressed more than Embigin at all three time points, and Embigin had the lowest level of expression throughout the mouse lifetime.

The highest level of Basigin expression was observed in one-month brain tissue. Expression levels in adult tissues decreased compared to the one-month tissue, but then leveled in adulthood (Figure 3.5). A statistically significant decrease in Basigin expression was observed between the one-month and six-month tissue ($P < 0.05$ by paired t-test) and between the one-month and twelve-month tissues ($P < 0.05$ by Student's t-test). A comparison between the six-month and twelve-month tissue samples showed a trend of increasing Basigin expression in aged mice, however, no statistically significant differences were noted ($P > 0.05$ by Student's t-test).

Like the other members of the Basigin subset, Embigin expression was highest in the one-month tissue and decreased in the adult tissue. Embigin

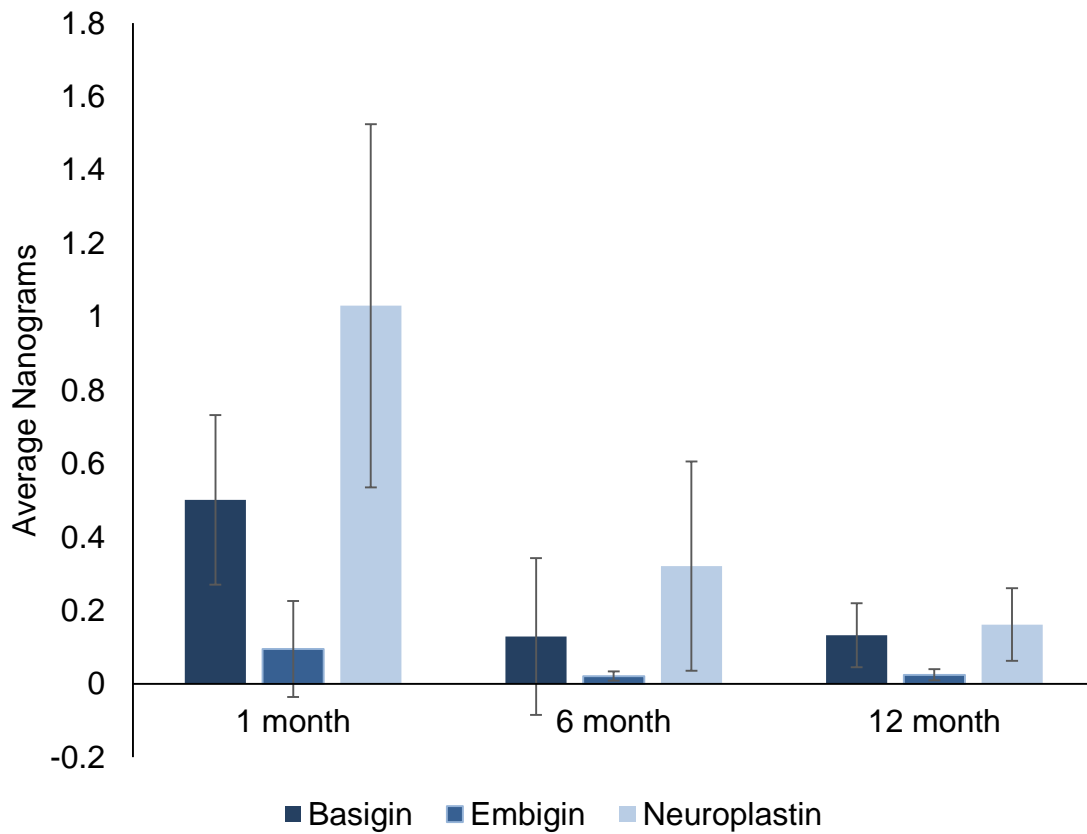


Figure 3.4 Comparison of Basigin, Neuroplastin, and Embigin expression. Tissue was isolated via an accepted protocol at the ages indicated and RNA was isolated for use in quantitative reverse transcription polymerase chain reaction (q-RT-PCR) using primer sets specific for Basigin gene products, Neuroplastin gene products, and Embigin. The values obtained were normalized to 18s RNA. All runs were performed in triplicate using 100 ng total RNA, and the average nanograms of RNA was plotted. Error bars represent the coefficient of variance. The melt curves indicated that a single product was obtained for each primer set (data not shown).

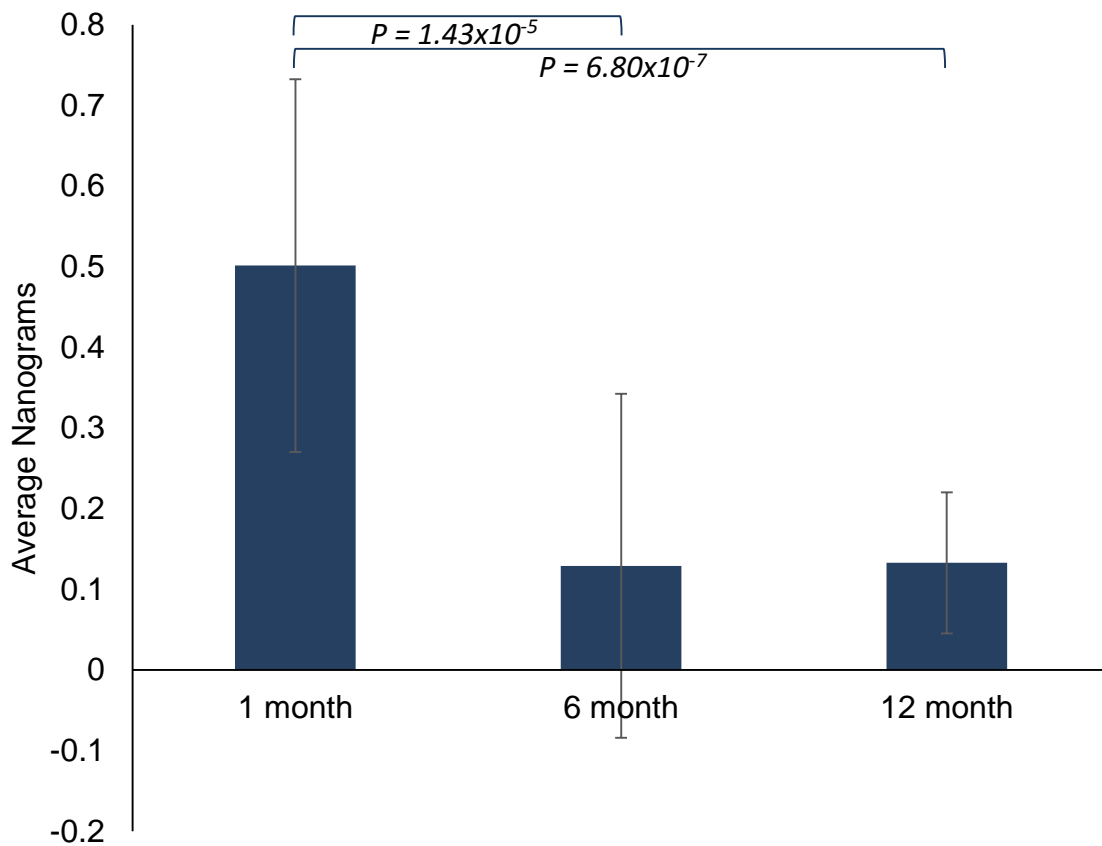


Figure 3.5 Comparison of Basigin expression over the mouse life span. Tissue was isolated via an accepted protocol at the ages indicated and RNA was isolated for use in quantitative reverse transcription polymerase chain reaction (q-RT-PCR) using primer sets specific for Basigin gene products. The values obtained were normalized to 18s RNA. All runs were performed in triplicate using 100 ng total RNA and the average nanograms of RNA was plotted. Error bars represent coefficient of variance. Significant difference between samples is indicated by the presence of bracket shown above and the corresponding *P* value. A melt curve analysis indicated that a single product was obtained (data not shown).

expression in adult tissue samples remained constant over time (Figure 3.6). The expression level of Embigin in one-month brain was more than four times higher than that of adult tissue. Embigin expression decreased significantly between one-month and six-month tissue and between one-month and twelve-month tissue ($P < 0.05$ by Student's t-test). No statistically significant differences were observed between the six-month and twelve-month adult tissues ($P > 0.05$ by Student's t-test).

The highest level of Neuroplastin expression was observed in one-month brain. Throughout development, expression levels of Neuroplastin decreased in an exponential pattern (Figure 3.7). A statistically significant decrease in Neuroplastin expression was observed between the one-month and six-month tissues ($P < 0.05$ by Student's t-test), the one-month and twelve-month tissues ($P < 0.05$ by paired t-test), and the six-month and twelve-month tissues ($P < 0.05$ by Student's t-test).

Expression of MCT-1 was also assessed in mouse brain. MCT-1 expression levels in tissues from each time point were minimal compared to the expression levels observed for the members of the Basigin subset (Table 3.1). MCT-1 expression was lowest in the six-month tissue and highest in the one-month tissue. A significant decrease in expression between one-month and six-month tissues ($P < 0.05$ by Student's t-test) and a significant increase in expression between the six-month and twelve-month tissues ($P < 0.05$ by Student's t-test) was observed for MCT-1 in brain. No differences between

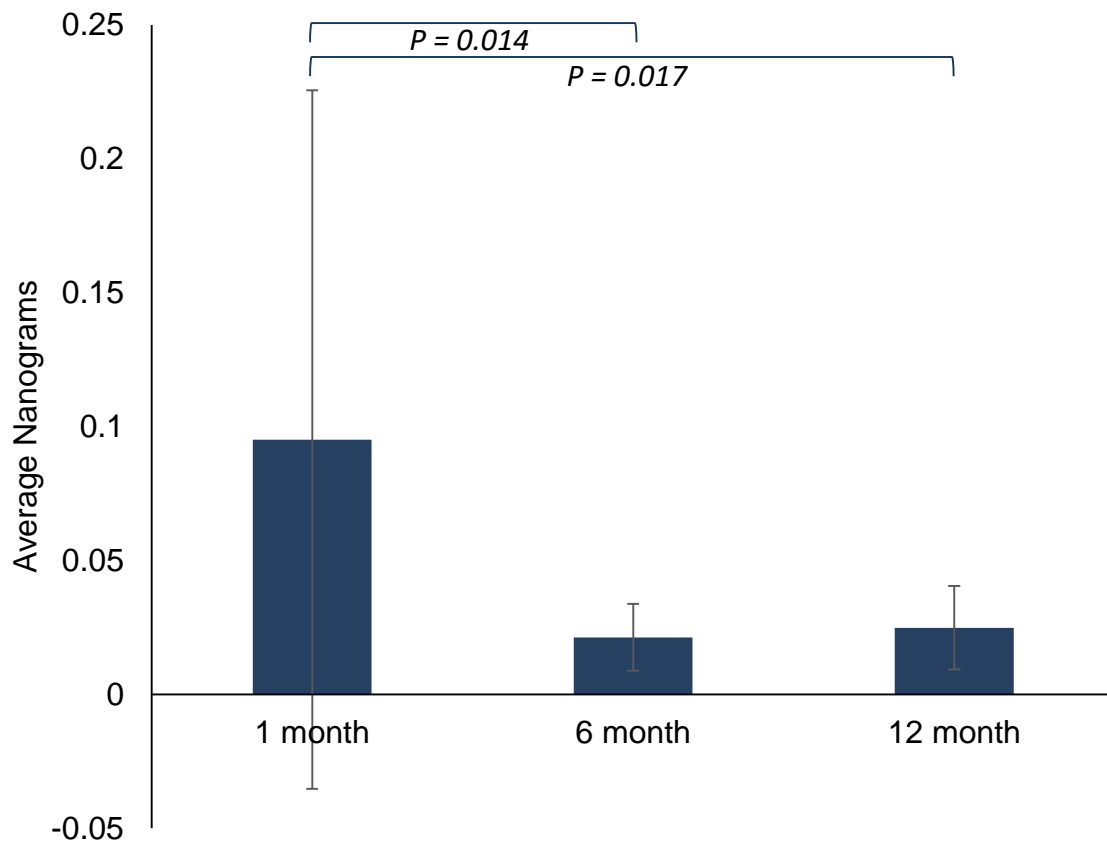


Figure 3.6 Comparison of Embigin expression over the mouse life span. Tissue was isolated via an accepted protocol at the ages indicated and RNA was isolated for use in quantitative reverse transcription polymerase chain reaction (q-RT-PCR) using primer sets specific for Embigin. The values obtained were normalized to 18s RNA. All runs were performed in triplicate using 100 ng total RNA and the average nanograms of RNA was plotted. Error bars represent the coefficient of variance. Significant difference between samples is indicated by the presence of bracket shown above and the corresponding *P* value. A melt curve analysis indicated that a single product was obtained (data not shown).

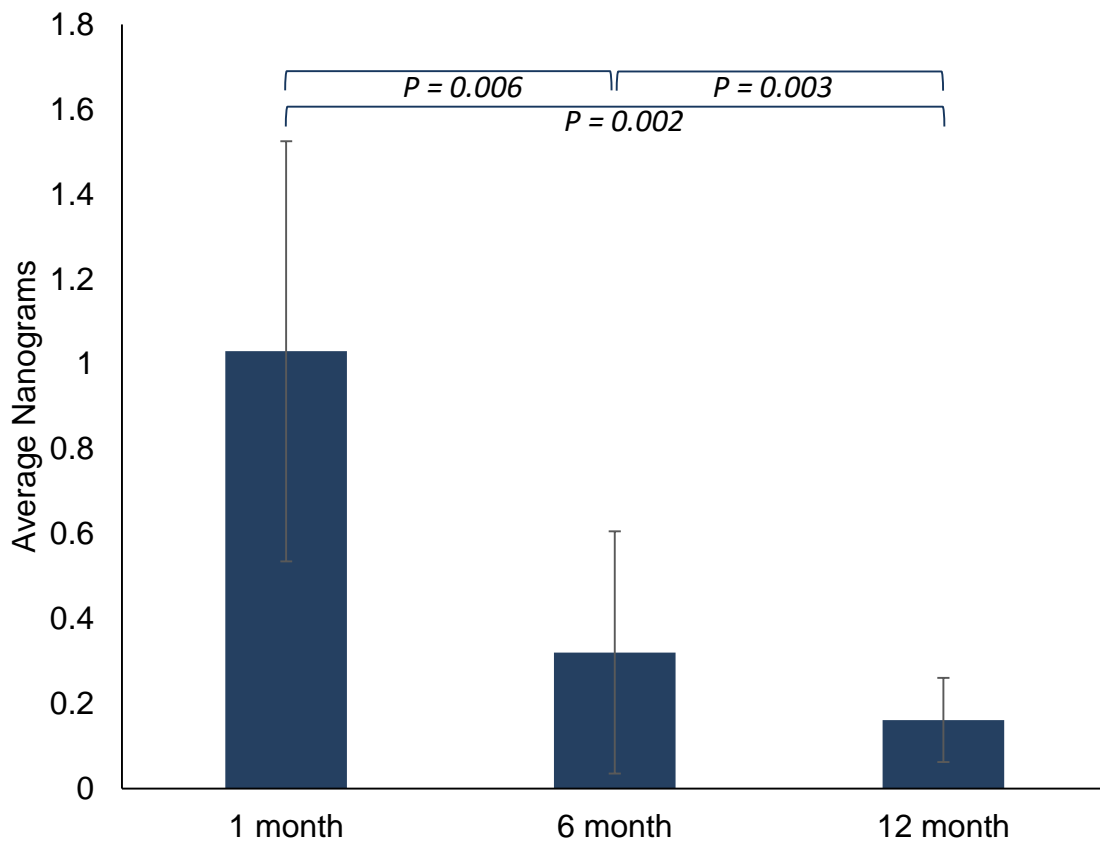


Figure 3.7 Comparison of Neuroplastin gene product expression over the mouse life span. Tissue was isolated via an accepted protocol at the ages indicated and RNA was isolated for use in quantitative reverse transcription polymerase chain reaction (q-RT-PCR) using primer sets specific for Neuroplastin gene products. The values obtained were normalized to 18s RNA. All runs were performed in triplicate using 100 ng total RNA and the average nanograms of RNA was plotted. Error bars represent the coefficient of variance. Significant difference between samples is indicated by the presence of bracket shown above and the corresponding *P* value. A melt curve analysis indicated that a single product was obtained (data not shown).

Table 3.1 Expression of monocarboxylate transporter 1 (MCT-1) in brain tissue over the mouse life span. Values represent average nanograms at the ages indicated. Statistically significant differences in expression compared to the six-month sample are indicated by the presence of an asterisk (*) and the corresponding *P* value. A melt curve analysis indicated that a single product was obtained (data not shown).

Brain Tissue		Average Nanograms	Variance	<i>P</i> value, $\alpha = 0.05$
1 month	*	2.06E-08	± 8.37E-06	0.014
6 month		2.37E-09	± 8.45E-07	
12 month	*	1.87E-08	± 5.26E-05	0.004

expression levels of MCT-1 in one-month and twelve-month brain samples were noted ($P < 0.05$ by paired t-test). MCT-1, although present in brain tissue, had expression levels that were smaller by several orders of magnitude compared to the expression levels of Basigin, Embigin, and Neuroplastin. The data collected indicated that MCT-1 was present in brain throughout the life of the mouse, albeit in diminutive amounts, and also indicated its expression decreases between one-month and six-month brain tissue then increases between six-month and twelve-month tissues.

Chapter 4 – Discussion

This study was the first to directly compare the expression of the three members of the Basigin subset of the IgSF in the mouse brain. In addition, the expression of MCT-1 was also assessed and compared to that of Basigin, Embigin, and Neuroplastin gene products. The study showed that expression levels of Neuroplastin were higher than those of Embigin or Basigin throughout the lifespan of the mouse, however, Neuroplastin exhibited a decrease in expression over time, especially in the aged animals. All Basigin subset members had highest levels of expression in the one-month tissue. Expression of Embigin and Basigin decreased in the adult tissues and leveled over time. Basigin had intermediate expression at all time points, while Embigin had the lowest level of expression. MCT-1 had relatively minute expression levels over time, but the highest level of expression was also observed in the one-month tissue sample.

The results of this study indicated that the Neuroplastin gene products have the highest expression of all the members of the Basigin subset for all the time points that were studied. The abundance of Neuroplastin in each tissue sample reinforces the hypothesis that it plays an important role in brain tissue throughout the entire life span of the mouse. Previous studies have indicated that Neuroplastin is involved in neurite outgrowth, synaptogenesis, and neuroplasticity (Beesley et al., 2014; Wilson et al., 2013; Owczarek et al., 2011),

Considering Neuroplastins' participation in these processes, their prevalence in brain tissue is expected, although their roles are not fully understood.

The highest level of Neuroplastin expression was observed in one-month brain tissue. Mice are considered to be developmentally mature at two-months of age (Silver, 1995), therefore, the one-month tissue samples were collected from mice still undergoing post-natal development. In rodents, synaptogenesis is most active between post-natal day seven and post-natal day thirty (O'Kusky et al., 2000). Because the brain tissue samples were collected from one-month mice nearing the end of highly active post-natal synaptogenesis, it is likely that the high levels of Neuroplastin levels observed in those tissues were due to higher levels of synaptogenic activity.

Although Neuroplastin had the highest expression of the Basigin subset members over time and high levels of expression were observed in one-month tissue, a significant decrease in expression was observed in all tissue samples over time. The statistically significant decrease in expression noted between the one-month and six-month tissues, the one-month and twelve-month tissues, and the six-month and twelve-month tissues suggests that expression of Neuroplastin decreased in an exponential pattern over the mouse life time. Synaptogenesis continues throughout adulthood, which contributes to plasticity and learning (Wiersma-Meems and Syed, 2006). It is possible that the decrease in Neuroplastin expression observed in mouse brain over time is associated with

decreased synaptogenesis and neural deficits that occur as result of aging, including learning and memory disorders seen in older individuals.

Neuroplastin is involved in neuroplasticity, a process which largely impacts learning and memory (Owczarek et al., 2010, Burgess et al., 2002). The hippocampus is the region of the brain that associated with memory and learning processes (Burgess et al., 2002). While Np65 is brain-specific and found throughout this tissue, higher levels of expression are found within the hippocampus (Wilson et al., 2013). Recent studies on geriatric mice with age-related reductions in neurogenesis have examined the effects of injecting fibroblast growth factors into the hippocampus to determine how they impact neurogenesis in the hippocampal region (Jin et al., 2003). The aged mice that were treated with a fibroblast growth factors demonstrated an increase in hippocampal neurogenesis and an ability to override suppression of neurogenesis (Jin et al., 2003).

The intracellular signaling pathway of long-form Neuroplastin is reliant on a fibroblast growth factor (Owczarek et al., 2011). As the levels of fibroblast growth factors decreases with age, it is possible that the Np65 signaling pathway is inhibited, resulting in decreased Neuroplastin expression as well as decreased synaptogenesis. Decreased fibroblast growth factor may also be related to suppression of neurogenesis, as was observed by the reduced neurogenesis in the geriatric mice in with an absence of fibroblast growth factor (Jin et al., 2003).

As a consequence of decreased Neuroplastin expression, the efficiency of synaptic activity would diminish, which would negatively impact neuroplasticity.

A decline in synaptic activity and neuroplasticity would result in compromised neural communication and result in associated neural deficits of decreased learning capabilities and memory loss. Loss of synaptic function is an early event in the progression of neural diseases such as Alzheimer's disease (Tchantchou et al., 2009). Therefore, the significant reduction in Neuroplastin expression with age may be related to the onset of dementia and could be a target for prevention of synapse loss and subsequent neural disease.

Embigin had the lowest level of expression of the Basigin subset at every studied time point that was studied. Because Embigin is the 'embryonic' immunoglobulin, it is expressed preferentially during gestational development and seen in lower levels at post-natal ages. The highest level of Embigin expression was observed in the one-month tissue. As indicated previously, a mouse is considered to be developmentally mature at two months of age (Silver, 1995), therefore, at one-month of age, the mouse is still undergoing post-natal development. Embigin levels are higher in developing tissues than in adult tissues, even if the adult tissue is undergoing post-natal development (Fan et al., 1998a). The low expression of Embigin in adult brain tissue over time suggests that it does not have an important function in mature brain tissue in the mouse.

Basigin, like the other members of the Basigin subset of the IgSF, had expression levels that were highest in one-month brain tissue. This suggests

that it may play a role in post-natal brain development. Expression levels of Basigin decreased significantly in adult tissue compared to one-month samples, suggesting a less important role in adult tissue. The intermediate levels of Basigin in this tissue suggest that it may perform functions necessary for normal brain function. Previous research has indicated that Basigin plays an important role in pain sensation, olfactory, and visual processes (Igakura et al., 1996; Naruhashi et al., 1997). Preliminary findings of studies on Neuroplastin null mice suggest that Basigin may play a compensatory role in the absence of functional Neuroplastin (K-H. Smalla, unpublished results).

A significant increase in MCT-1 expression was observed from six-month to twelve-month tissue, whereas Neuroplastin expression during this time period decreased significantly. The simultaneous increase of MCT-1 and decrease of Neuroplastin levels suggest that MCT-1 could be upregulated as a result of low Neuroplastin levels. It is possible that MCT-1 may be upregulated in an attempt to increase the transport of lactate to neurons. This could be further evidence of compensatory mechanisms that are stimulated by a decrease in Neuroplastin levels.

MCT-1 levels were highest in the one-month tissue, sample, but as previously stated, tissues from one month mice were in the end stages of post-natal development when they were isolated. Developing brain may have a metabolic demand that is higher than that of fully developed, mature brain tissue, which would explain the higher levels of MCT-1 observed in young brain tissue.

Throughout the mouse lifetime, observed MCT-1 levels in brain were consistently lower than the expression levels of the Basigin subset by several orders of magnitude. Consistently low MCT-1 expression levels indicate that it plays a less prominent role in brain tissue than in the neural retina. It is likely that low levels of MCT-1 expression were observed because MCT-1 is not the dominant monocarboxylate transporter in brain tissue.

Structurally and functionally related to MCT-1, MCT-2 is expressed in high levels throughout neural tissue (Halestrap, 2012). MCT-2 expression is not widely expressed like MCT-1, and the two are not typically co-expressed in tissues (Halestrap and Price, 1999; Halestrap, 2012). MCT-2 has a higher binding affinity for lactate than MCT-1, which facilitates the uptake of lactate for use as respiratory fuel in neurons and ensures their metabolic needs are met (Bergerson, 2007).

The MCT-1 levels observed in brain tissue might be in such small amounts because they are expressed only on the endothelial lining of blood vessels that comprise the blood-brain barrier. Previous studies show that MCT-1 has been found throughout the plasma membrane of endothelial cells in the blood brain barrier. This indicates that MCT-1 plays an important role in supplying the brain with lactate, although perhaps not within the neural tissue itself. (Gerhart et al., 1997)

Chapter 5 – Conclusions

The purpose of this study was to quantify the expression levels of the Basigin subset of the Immunoglobulin Superfamily and MCT-1 in brain over the course of the mouse lifetime using q-RT-PCR and to identify any changes in expression patterns that occur throughout that time. High levels of Neuroplastin were found throughout the lifespan, but levels decreased exponentially over time. All three members of the Basigin subset and MCT-1 had the highest expression levels in the youngest mouse tissue. Both Basigin and Embigin levels decreased and remained constant in adult tissues. Basigin had intermediate expression, whereas Embigin had the lowest level of expression. MCT-1 levels remained low in mouse over time, but had the lowest expression level in the six-month sample.

From this study, it can be inferred that Neuroplastin plays an important role in neural tissue, which was demonstrated by high levels of expression throughout the life span. Decreased Neuroplastin levels over time could be associated with neural deficits that are seen in older individuals. Down regulation of Neuroplastin expression could result in diminished neural communication because synaptic strength breaks down over time or because cellular adhesion events crucial to normal function are no longer occurring. This hypothesis is supported by the upregulation of MCT-1 in tissues with low Neuroplastin expression and suggests the presence of compensatory mechanisms to allow continuation of proper brain function. To further understand the role that Neuroplastin may play in the cerebral lactate metabolon, the Ochrietor lab will

analyze the binding affinity of Neuroplastin for MCT-2 to see if these molecules contribute to metabolic activity within the brain.

The information generated from this study contributes to the knowledge of the Basigin subset of the IgSF in the brain, as well the understanding of overall brain function. The novel results from this study provide information that furthers the growing understanding Neuroplastin function and assist in determining the role of Neuroplastin in the proposed cerebral lactate metabolon. The relationship between Neuroplastin expression and neural deficits seen in older individuals should be further studied to see if low levels of Neuroplastin cause dementia, result from dementia, or are entirely unrelated. If a positive link between memory disorders and decreased Neuroplastin expression can be identified, regulating Neuroplastin expression may be a potential target for preventing loss of synaptic function, memory loss, and neural disorders.

References

- Bear, M.F., Connors, B.W., and Paradiso, M.A. *Neuroscience: exploring the brain*. Baltimore, MD: Lippincott Williams & Wilkins. (2007): 2nd edition.
- Beesley, P.W., Herrera-Molina, R., Smalla, K., and Seidenbecher, C. The Neuroplastin adhesion molecules: key regulators of neuronal plasticity and synaptic function. *J Neurochem*. 131 (2014): 268-283.
- Bergersen, L.H. Is lactate food for neurons? Comparison of monocarboxylate transporter subtypes in brain and muscle. *Neurosci*. 145.1 (2007): 11-19.
- Bouzier-Sore, A., Canioni, P., Magistretti, P.J., and Pellerin, L. Lactate is a preferential oxidative energy substrate over glucose for neurons in culture. *J Cereb Blood Flow Metabo*. 23.11 (2003): 1298-1306.
- Burgess, N., Maguir, E.A., and O'Keefe, J. The human hippocampus and spatial and episodic memory. *Neuron*. 35 (2002): 625-641
- Clamp, M. F., Ochrietor, J. D., Moroz, T. P., and Linser, P. J. Developmental analyses of 5A11/Basigin, 5A11/Basigin-2 and their putative binding partner MCT1 in the mouse eye. *Exp Eye Res*. 78.4 (2004): 777-89.
- Daniel, P.M., Love, E.R., and Pratt O.E. The transport of ketone bodies into the brain of the rat (*in vivo*). *J Neuro Sci*. 34.1 (1977): 1-13.
- Demetrius, L.A., Magistretti, P.J., and Pellerin, L. Alzheimer's disease: the amyloid hypothesis and the inverse Warburg effect. *Front Physiol*. 5 (2015): 1-20.
- Fan, Q., Yuasa, S., Kuno, N., Senda, T., Kobayashi, M., Muramatsu, T., and Kadomatsu, K. Expression of Basigin, a member of the Immunoglobulin Superfamily, in the mouse central nervous system. *Neurosci Res*. 30 (1998): 53-63.
- Fan, Q.W, Kadomatsu, K., Uchimura, K., and Muramatsu, T. Embigin/Basigin Subgroup of the Immunoglobulin Superfamily: different modes of expression during mouse embryogenesis and correlated expression with carbohydrate antigenic markers. *Dev Growth Differ*. 40 (1998b): 277-86.

- Finch, N.A., Linser, P.J., and Ochrietor, J.D. Hydrophobic interactions stabilize the Basigin-MCT1 complex. *Spring Sci+Bus Med.* 28 (2009): 362-368.
- Gambon, P.L. Localization and characterization of the interactions between Basigin gene products and Monocarboxylate Transporters in the olfactory bulb of the mouse. *UNF Theses and Dissertations.* (2011): Paper 126.
- Demetrius, L.A., Magistretti, P.J., and Pellerin, L. Alzheimer's disease: the amyloid hypothesis and the Inverse Warburg effect. *Front Physiol.* 5 (2015): 1-20.
- Gerhart, D.Z. and Enerson, B.E. Expression of monocarboxylate transporter MCT1 by brain endothelium and glia in adult and suckling rats. *Am J Physiol.* 273.1 (1997): E207-E213.
- Guenette, R.S., Sridhar, S., Herley, M., Mooibroek, M., Wong, P., and Tenniswood, M. Embigin, a developmentally expressed member of the Immunoglobulin Super Family, is also expressed during regression of prostate and mammary gland. *Dev Gen.* 21.4 (1997): 268-78.
- Halaby, D.M. and Mornon, J.P.E. The Immunoglobulin Superfamily: an insight on its tissular, species, and functional diversity. *J Mole Evol.* 46 (1998): 389-400.
- Halestrap, A.P. The monocarboxylate transporter family –structure and functional characterization. *IUBMB Life.* 64 (2012): 1-9.
- Halestrap, A.P. and Price N.T. The proton-linked monocarboxylate transporter (MCT) family: structure, function and regulation. *J Biochem.* 343(1999): 281-299.
- Halestrap, A.P. and Wilson, M.C. The monocarboxylate transporter family – role and regulation. *IUBMB.* 64.2 (2012): 109-119.
- Hori, A., Katayama, N., Kachi, S., Kondo, M., Kadomatsu, K., Usukura, J., Muramatsu, T., Mori, S., and Miyake Y. Retinal dysfunction in Basigin deficiency. *IOVS.* 41 (2000): 3128-3133.
- Howard, J., Finch, N.A., and Ochrietor, J.D. Characterization of monocarboxylate transporter 1 (MCT1) binding affinity for Basigin gene products and L1cam. *Cell Mol Neurobiol.* 30 (2010): 671-674.

- Huang, R.P., Ozawa, M., Kadomatsu, K., and Muramatsu, T. Developmentally regulated expression of Embigin, a member of the Immunoglobulin Superfamily found in embryonal carcinoma cells. *Diff Ontogeny Neoplasia*. (1990): 76-83.
- Igakura, T., Kadomatsu, K., Kaname, T., Muramatsu, H., Fan, Q.W., Miyauchi, T., Toyama, Y., Kuno, N., Yuasa, S., Takahashi, M., Senda, T., Taguchi, O., Yamamura, K., Arimura, K., and Muramatsu, T. A null mutation in Basigin, an Immunoglobulin Superfamily member, indicates its important roles in peri-implantation development and spermatogenesis. *Dev Biol*. 194 (1998): 152-165.
- Igakura, T., Kadomatsu, K., Taguchi, O., Muramatsu, H., Kaname, T., Miyauchi, T., Yamamura, K., Arimura, K., and Muramatsu, T. Roles of Basigin, a member of the Immunoglobulin Superfamily, in behavior as to an irritating odor, lymphocyte response, and blood-brain barrier. *Biochem Biophys Res Commun*. 224 (1996): 33-36.
- Itoh, Y., Esaki, T., Shimoji, K., Cook, M., Law, M., Kaufman, E., and Sokoloff, L. Dichloroacetate effects on glucose and lactate oxidation by neurons and astroglia in vitro and on glucose utilization by brain in vivo. *PNAS*. 100.8 (2003): 4879-884.
- Jin, K., Yunjuan, S., Xie, L., Batteur, S., Ou Mao, X., Smelick, C., Logvinova, A., and Greenberg, D.A. Neurogenesis and aging: FGF-2 and HB-EGF restore neurogenesis in hippocampus and subventricular zone of aged mice. *Aging Cell*. 2 (2003): 175-183.
- Kanekura, T. and Chen, X. CD147/Basigin promotes progression of malignant melanoma and other cancers. *J Dermatol Sci*. 57 (2010): 149-154.
- Kirk, P., Wilson, M.C., Heddle, C., Brown, M.H., Barclay A.N., Halestrap, A.P. CD147 is tightly associated with lactate transporters MCT1 and MCT4 and facilitates their cell surface expression. *Euro Mol Bio J*. 19 (2000): 3896-3904.
- Lain, E., Carnejac, S., Escher, P., Wilson, M.C., Lomo, T., Gajendran, N., and Brenner, H.R. A novel role for Embigin to promote sprouting of motor nerve terminals at the neuromuscular junction. *J Biol Chem*. 284 (2009): 8930-8939.

- Langnaese, K., Beesley, P.W., and Gundelfingers, E.D. Synaptic membrane glycoproteins gp65 and pg55 are new members of the Immunoglobulin Superfamily. *J Bio Chem.* 272.2 (1997): 821-827
- Little, L.N. Characterization of Basigin and the interaction between Embigin and Monocarboxylate Transporter-1, -2, and -4 (MCT1, MCT2, MCT4) in the mouse brain. *UNF Theses and Dissertations.* (2011): Paper 170.
- Llano-Diez, M., Gustafson, A.M., Olsson, C., Goransson, H., and Larsson, L. Muscle wasting and the temporal gene expression pattern in a novel rat intensive care unit model. *BMC Genomics.* 12 (2011): 602-616.
- Lodish, H., Berk, A., Zipursky, S.L., Matsudaira, P., Baltimore, D., and Darnell, J. *Molecular Cell Biology.* New York: W.H. Freeman. (2000): 4th edition.
- Miyauchi, T., Masuzawa, Y., Muramatsu, T. The Basigin group of the Immunoglobulin Superfamily: complete conservation of a segment in and around transmembrane domains of human and mouse Basigin and chicken HT7 antigen. *J Biochem.* 110 (1991): 770-774.
- Nakai, M., Chen, L., and Nowak R.A. Tissue distribution of Basigin and Monocarboxylate Transporter 1 in the adult male mouse: a study using the wild-type and Basigin gene knockout mice. *Anat Rec.* 288.A (2006): 527-35.
- Naruhashi, K., Kadomatsu, K., Igakura, T., Fan, Q., Kuno, N., Muramatsu, H., Miyauchi, T., Hasegawa, T., Itoh, A., Muramatsu T., and Nabeshima, T. Abnormalities of sensory and memory functions in mice lacking Basigin gene. *Biochem Biophys Res Comm.* 236.3 (1997): 733-737.
- O'Kusky, J.R., Ye, P., and D'Ercole, A.J. Insulin-Like Growth Factor-1 promotes neurogenesis and synaptogenesis in the hippocampal dentate gyrus during postnatal development. *J Neurosci.* 20.22 (2000): 8435-8442.
- Ochrietor, J.D. and Linser, P.J. 5A11/Basigin gene products are necessary for proper maturation and function of the retina. *J Dev Neurosci.* 26 (2004): 5-6.
- Ochrietor, J.D., Moroz, T., Clamp, M., Timmers, A., Muramatsu, T., and Linser, P. Inactivation of the Basigin gene impairs normal retinal development and maturation. *Vis Res.* 42.4 (2002): 447-53.

- Ochrietor, J.D., P. Moroz, T., Ekeris, L.V., Clamp, M.F., Jefferson, S.C., DeCarvalho, A.C., Fadool, J.M., Wistow, G., Muramatsu, T., and Linser, P.J. Retina-specific expression of 5A11/Basigin-2, a member of the Immunoglobulin Gene Superfamily. *IVOS*. 44.9 (2003): 4086-096.
- Ochrietor, J., Moroz, T. M., Kadomatsu, K., Muramatsu, T., and Linser, P.J. Retinal degeneration following failed photoreceptor maturation in 5A11/Basigin Null Mice. *Exp Eye Res*. 72.4 (2001): 467-77.
- O'Kusky, J.R., Ye, P., D'Ercole, A.J. Insulin-Like Growth Factor-1 promotes neurogenesis and synaptogenesis in the hippocampal dentate gyrus during postnatal development. *J Neurosci*. 20:22 (2000): 8435-8442.
- Owczarek, S., Kiryushko, D., Larsen, M.H., Kastrup, J.S., Gajhede, M., Sandi, C., Berezin, V., Bock, E., and Soroka, V. Neuroplastin-55 binds to and signals through the fibroblast growth factor receptor. *FASEB J*. 24 (2010): 1139-1150.
- Owczarek, S., Soroka, V., Kiryushko, D., Larsen, M.H., Yuan, Q., Sandi, C., Berezin, V. and Bock, E. Neuroplastin-65 and a mimetic peptide derived from its homophilic binding site modulate neuritogenesis and neuronal plasticity. *J Neurochem*. 117 (2011): 984-994.
- Ozawa, M., Huang, R.P., Furukawa, T., and Muramatsu, T. A teratocarcinoma glycoprotein carrying a developmentally regulated carbohydrate marker is a member of the immunoglobulin gene superfamily. *J Biol Chem*. 263 (1988): 3059-3062.
- Pellerin, L. How astrocytes feed hungry neurons. *Mole Neurobio*. 32.1 (2005): 59-72.
- Philp, N.J., Ochrietor, J.D., Rudoy, C., Muramatsu, T., and Linser, P.J. Loss of MCT1, MCT3, and MCT4 expression in the retinal pigment epithelium and neural retina of the 5A11/Basigin-null mouse. *IVOS*. 44.3 (2003a): 1305-311.
- Philp, N.J., Wang, D., Yoon, H., and Hjelmeland, L. Polarized expression of monocarboxylate transporters in human retinal pigment epithelium and ARPE-19 Cells. *IOVS*. 44 (2003b): 1716-1721.

- Redzic, J.S., Armstrong, G.S., Isern, N.G., Jones, D.N.M., Kieft, J.S., and Eisenmesser, E.Z. The retinal specific CD147 Ig0 domain: from molecular structure to biological activity. *J Mol Biol.* 411 (2011): 68-82.
- Shen, K. Molecular mechanisms of target specificity during synapse formation. *Curr Opin Neurobiol.* 14 (2004): 83-88.
- Sievers, F., Wilm, A., Dineen, D.G., Gibson, T.J., Karplus, K., Li, W., Lopez, R., McWilliam, H., Remmert, M., Söding, J., Thompson, J.D., and Higgins, D.G. Fast, scalable generation of high-quality protein multiple sequence alignments using Clustal Omega. *Molecular Systems Biology.* 7 (2011): 539.
- Silver, L.M. Reproduction and Breeding. *Mouse Genetics: Concepts and Applications.* New York, NY: Oxford University Press. (1995): 1st edition.
- Suzuki, A., Stern, S.A., Bozdagi, O., Huntley, G.W., Walker, R.H., Magistretti, P.J., and Alberini, C.M. Astrocyte-neuron lactate transport is required for long-term memory formation. *Cell.* (2011): 810–823.
- Tchantchoua, F. Lacorb, P.N., Caoa, Z., Laoc, L., Houd, Y., Cuie, C., Klein, W.L., and Luo, Y. Stimulation of neurogenesis and synaptogenesis by bilobalide and quercetin via common final pathway in hippocampal neurons. *J Alzheimers Dis.* 18 (2009): 787-798.
- Toyama, Y., Maekawa, M., Kadomatsu, K., Miyauchi, T., Muramatsu, T., and Yuasa, S. Histological characterization of defective spermatogenesis in mice lacking the Basigin gene. *Anat Histol Embryol.* 28 (1999): 205-13.
- Tsacopoulos, M. and Magistretti, P.J. Metabolic coupling between glia and neurons. *J Neurosci.* 16 (1996): 877-885.
- Vannucci, R.C. and Duffy, T.E. Influence of birth on carbohydrate and energy metabolism in rat brain. *Am J Phys.* 226 (1974): 933-40.
- Wiersma-Meems, R. and Syed, N.I. Synapse formation between identified molluscan neurons: a model system approach. *Molecular Mechanisms of Synaptogenesis.* New York, NY: Spring Sci+Bus Med (2006): 29-42.
- Williams, A.F. A year in the life of the immunoglobulin superfamily. *Immunol Today.* 8 (1987): 298-303.

- Wilson, M.C., Meredith, D., and Halestrap, A.P. Fluorescence Resonance Energy Transfer studies on the interaction between the lactate transporter MCT1 and CD147 provide information on the topology and stoichiometry of the complex in situ. *J Biol Chem.* 277.5 (2002): 3666-3672.
- Wilson, M.C., Meredith, D., Bunnun, C., Sessions, R.B., and Halestrap, A.P. Studies on the DIDS-binding Side of Monocarboxylate Transporter 1 Suggest a Homology Model of the Open Conformation and a Plausible Translocation Cycle. *J Bio Chem.* 284.30 (2009): 20011-20021.
- Wilson, M.C., Kraus, M., Marzban, H., Sarna, J.R., Wang, Y., Hawkes, R., Halestrap, A.P., and Beesley, P.W. The Neuroplastin adhesion molecules are accessory proteins that chaperone the monocarboxylate transporter MCT2 to the neuronal cell surface. *PLoS ONE.* 8 (2013): 1-9.
- Yan, L., Zucker, S., and Toole, B.P. Roles of the multifunctional glycoprotein, EMMPRIN (Basigin; CD147), in tumor progression. *Thromb Haemost.* 93 (2005): 199-204.

Vita

AUTHOR: Tavia N. Hall

EDUCATION:

Bachelor of Science in Biology – Biomedical Sciences
University of North Florida, Jacksonville, FL, Expected 2016

RELEVANT EXPERIENCE:

Resident Assistant, University of North Florida, 2014-2015
Academic Tutor, Poplar Bluff R1 School System, 2009-2011

HONORS AND AWARDS:

Osprey Student Scholar Award, 2016
Biology Research Award Nominee, 2016
University of North Florida Transformational Learning Opportunity
Scholarship Recipient, 2016
University of North Florida Student Mentored Academic Research Team
Grant Recipient, 2015
Missouri University of Science and Technology Research Conference
1st Place Recipient, 2012
International Genetically Engineered Machine Design Team
Scholarship Recipient, 2012
Missouri University of Science and Technology
Trustee's Scholarship Recipient, 2011

PRESENTATIONS:

T.N. Hall and J.D. Ochrietor

Analysis of the Basigin subset of the Immunoglobulin Superfamily in the mouse brain over time.
Showcase of Osprey Achievements in Research and Scholarship 2016
Jacksonville, FL. Oral Presentation.

T.N. Hall and J.D. Ochrietor

Analysis of the Basigin subset of the Immunoglobulin Superfamily in the mouse brain over time.
Experimental Biology 2016, American Society for Biochemistry and Molecular Biology Undergraduate Research Competition 2016, San Diego, CA. Poster Presentation, Published Abstract.

T.N. Hall and J.D. Ochrietor

Analysis of the Basigin subset of the Immunoglobulin Superfamily in the adult mouse brain over time.

Florida Undergraduate Research Conference 2016, Tampa FL. Poster Presentation.

T.N. Hall and D.J. Westenberg

Biodesign of *Asaia* to interrupt the lifecycle of *Plasmodium falciparum* in *Anopholes*.

Missouri University of Science and Technology Undergraduate Research Conference 2012, Rolla, MO. Poster Presentation.